Journal of Data Acquisition and Processing
ISSN: 1004-9037
https://sjcjycl.cn/
DOI: 10.5281/zenodo.777917

SPATIAL DISTRIBUTION OF TRACE ELEMENT CA-NORMALIZED RATIOS IN BONE AFTER ACUTE ORAL ADMINISTRATION OF LA_2O_3NPs.

Oluwafemi Temitayo Ogunmodede[1*], Ogola-Emmal Ebitimitula[2], Kolawole Sunday[3], Valderi Luiz Dressler[4]

[1*]Department of Chemical Sciences, Afe Babalola University Ado-Ekiti, P.M.B, Ado-Ekiti 5454, Nigeria

[2]Department of Chemistry, Bayelsa Medical university, P.M.B. 178, Yenagoa, Nigeria

[3]Department of Chemistry, University of Abuja, Nigeria

[4]Departamento de Química, Universidade Federal de Santa Maria, Santa Maria, RS 97105-900, Brazil

***Corresponding Author:** Oluwafemi Temitayo Ogunmodede

E-mail address: ogunmodedeo@abuad.edu.ng

Abstract

The trace elements distribution embedded in bone offers a means to study exposure of toxic metals and allows the reconstruction of dietary behaviour. The quantification of most of the elements with a spatial high resolution (5 μm) is routinely achieved using laser ablation inductively coupled plasma mass spectrometry (LA-ICP-MS). However, the lack of a comprehensive framework of trace elements distribution in bone jeopardizes any endorsed sampling strategy using LA-ICP-MS. The present work is an effort to improve our knowledge on this issue. We studied a femur bone head treated with La_2O_3NPs at 1.0 mg kg^{-1} (T1), 10.0 mg kg^{-1} (T2), and 100 mg kg^{-1} (T3) body weight (bw) and the control rats (CTR). Using LA-ICP-MS, we measured Ca, Cu, Zn, Ni, Sr, Ba and Pb in a cross section of the femur bone head, where higher amounts of the elements are present at the external part of the bone. Calcium concentrations are higher in control than in the La_2O_3NPs treated bone. The Pb/Ca, Cu/Ca, Ni/Ca, Zn/Ca, Sr/Ca and Ba/ Ca ratios were higher in control femur head but vary within T_1, T_2 and T_3 body weight (bw). Considering the Ca-normalized bone variations of Pb, Cu, Ni, Zn, Sr and Ba, it was demonstrated that La_2O_3NPs are incorporated on the surface of the bone and it has a small influence on some of the other elements evaluated.

Keywords: Bone, Laser ablation, Strontium, Barium, Bio-imaging, Nanoparticle

1.0 Introduction

Bone formation and growth is controlled by a complex array of feedback processes that depends on several biological and environmental factors (i.e. exposure to toxicants). A number of toxicological studies have demonstrated that bone tissue is highly sensitive to many types of toxic substances (i.e., heavy metals, organochlorine compounds) which affect bone composition and mineralization, producing specific bone abnormalities and pathologies [1, 2, 3]. Healthy bone is a mineralized connective tissue composed by water, an organic phase (mainly collagen type I) which surrounds the mineral crystals, and an inorganic part best approximated as hydroxyapatite [Hap] ($Ca_{10}(PO_4)_6(OH)_2$), that makes about a quarter of the bone volume and 60–70% of dry weight of adult normal bone. The fraction of calcium in hydroxyapatite is 39.9%, phosphorous 18.5% and the Ca/P ratio is 2.2 [4, 5]. Hydroxyapatite

is composed of various elements, covering nearly 50% of the elements in the periodic table. Among these, a number of metal cations (e.g. Mg^{2+}, Sr^{2+}, Zn^{2+}, Na^{+} and K^{+}) are present in biological HAp by substituting Ca^{2+}, and anions (e.g. CO_3^{2-}, F^{-} and Cl^{-}) are present by substituting PO_4^{3-} or OH^{-}. The major substituting ions in the biological HAp are CO_3^{2-} (7.4%), Na^{+} (0.9%), Mg^{2+} (0.72%), K^{+} (0.03%), F^{-} (0.03%) and Cl^{-} (0.13%), [6] whereas trace elements, such as Fe^{2+}, Zn^{2+} and Sr^{2+}, can be also found in biological HAp. [7] It should be noted that the substitution of PO_4^{3-} by CO_3^{2-} (B-type substitution) [8] produces lattice vacancies on both Ca^{2+} and OH^{-} sites to compensate for the charge difference between PO_4^{3-} and CO_3^{2-} [9]. This is also true for the substitutions of Ca^{2+} by monovalent (Na^{+}, K^{+}) or trivalent (Al^{3+}, Fe^{3+}, La^{3+}) cations [10, 11]. Biological apatite found in bone, enamel or dentin is often referred to as hydroxyapatite (HAp: $Ca_{10}(PO_4)_6(OH)_2$) [12].

For vertebrate animals, the bone has an important role in the regulation of the concentrations of several essential inorganic nutrients, such as P, Ca, and Mg, in the cell or biological fluids [13, 14]. Calcium is one of the chemical elements essential to human beings, with which the normal functions of the cardiovascular, neuromuscular, and central nervous systems are associated. In their sizes, bonding, coordination geometry and donor atom preference, lanthanide ions (La^{3+}) are remarkably similar to Ca^{2+}, which permits La^{3+} to occupy Ca^{2+}-binding sites. But due to their higher valency, La^{3+} should behave much stronger binding ability than Ca^{2+}, [15]. Therefore, the existence of La^{3+} will affect most of membrane transport processes involving Ca^{2+}. For example, when applied extracellularly, La^{3+} can inhibit plasma membrane Ca^{2+} pumps [16], capacitative Ca^{2+} entry, Na^{+}/Ca^{2+} exchange [17].

The trace elements distribution embedded in bone represents an archive of the environmental conditions that prevailed when the bone was forming, but this information needs to be deciphered using appropriate techniques. Since the first study published around 1995 [18], laser ablation hyphenated to inductively coupled plasma mass spectrometer (LA-ICP-MS) is becoming increasingly utilized for analyzing tooth enamel and bone in toxicological and archaeological sciences. Two main reasons explain this keen interest. The first is linked to the ICP-MS capabilities, such as large linear response, low limits of detection (bμg/g) and multi-elemental analysis [19]. The second reason is that enamel has an incremental structure that allows the spatial reconstruction of chemical variations in relation to growth patterns [20]. Three main avenues of research are currently analyzing teeth and bone with LA- ICP-MS: toxicology, paleo-biology and diagenesis. Exposure of toxic metals, such as Pb, and further incorporation in the body can be monitored by analyzing bone and tooth enamel levels and spatial distribution [21, 22, 23, 24, 26, 27]. Ingestion of metals that are segregated by mammal metabolism, such as Sr and Ba, and whose dietary level dramatically change during weaning, can be reconstructed by analyzing spatial variations in bone and tooth enamel [28, 29, 30, 31, 32, 33].

A concern for studying the chemical composition of bone and tooth enamel by means of LA-ICP-MS is to decipher chemical variations linked to age related changes from those generated by bone formation and dental growth. Ideally, bone and teeth must be sectioned to have a flat surface suitable for the laser ablation technique. It is in some cases however impossible, like for precious fossil samples such as hominins teeth. The laser ablation is thus performed on the surface of the bone and teeth enamel but this can lead to instrumental elemental and isotopic

fractionation because the laser can be unfocused if the surface is too curved. Working with laser ablation on the surface of a tooth can yield accurate but locally restricted results [34], which can be problematic for highly variable parameter such as the $^{87}Sr/^{86}Sr$ ratio [35]. An alternative is to work on broken bone and perform the ablation profiles along the crack [36]. Nowadays, it is possible to obtain, thanks to big data computing, a full bio-image of concentrations [37, 38, 39, 40]. The results are usually impressive, but the technique is still highly time consuming (and as consequence expensive), even if the bio-image is interpolated from a grid of spots.

In conclusion, there is still a need for a fast and reliable strategy to analyze bone by means of LA-ICP-MS. In the present work, we have analyzed the effect of La_2O_3NPs on calcium (Ca), copper (Cu), zinc (Zn), nickel (Ni), strontium (Sr), barium (Ba) and lead (Pb) after administration of La_2O_3NPs to rats during 30 days. Different doses of NPs were administered to the animals by gavage. We propose that the most suitable location to perform laser ablation profile is along the femur head, because this area retains most of the information without significant attenuation.

2.0 Materials and Methods

This study was performed on the time course and effects of the incorporation/efflux of lanthanum into/out of bone. Out of the 30 available bone samples, 12 were selected according to the bone lanthanum content and bone histology.

2.1 Reagents and Standards

La_2O_3 nanoparticles were purchased from Nanoamor (Houston, USA), with 99.9% purity. Water was distilled, de- ionized, and then purified to obtain 18.2 MΩ cm resistivity (Milli-Q system, Millipore corp., Bedford, USA). Concentrated HNO_3 (65%, Merck, Darmstadt, Germany) was purified using a sub-boiling system (Milestone, Model Duopor, Bergamo, Italy). A multi-element standard solution containing 10 mg L^{-1} of each element (SCP33MS, SCP Science, Quebec, Canada) was used to prepare calibration solutions in the range of 0.025 to 10 μg L^{-1} for PN-ICP-MS and 5 to 100 μg L^{-1} for ICP OES. A multi-elemental standard (Merck) with concentration ranging from 0.1 to 10 mg L^{-1} of Ca, Mg, S, P, K, and Na was used for determination of elements with higher concentration by ICP OES. La_2O_3NP suspensions were prepared in purified water, sonicated in an ultrasonic bath for 10 min and immediately administered to the animals.

2.2 Animals

Male Wistar rats (200 to 290 g at the start of the experiment (N = 30) at 60 days of age) were acquired from Biotério Central of Universidade Federal de Santa Maria, Santa Maria, Brazil. Before submitting it to La_2O_3NP treatment, the animals spent a period of 7 days of adaption in a group of five in polypropylene cages. The animals were acclimatized under standard conditions of temperature (23°C ± 1), 50 to 60% relative humidity, and 12 h light/12 h dark cycles. The food and water were provided ad lib. Rat standard diet was used to feed the animals which contains the basic components for the animal diet. The food was acquired from Alisul Alimentos Brazil (Supra), which informed composition is moisture (max) 120 g kg^{-1} (12%),

crude protein (min) 220 g kg^{-1} (22%), ether extract (min) 25 g kg^{-1} (2.5%), fibrous matter (max) 60 g kg^{-1} (6%), mineral matter (max) 100 g kg^{-1} (10%), Ca 8000–12000 mg kg^{-1} (0.8–1.2%), P (min) 7000 mg kg^{-1} (0.7 %), methionine (min) 3000 mg kg^{-1}, vitamin A (min) 7000 UI kg^{-1}, vitamin C (min) 50 mg kg^{-1}, vitamin D_3 (min) 2000 UI kg^{-1}, vitamin E (min) 15 UI kg^{-1}, vitamin K_3 (min) 1 mg kg^{-1}, vitamin B_1 (min) 2 mg kg^{-1}, vitamin B_2 (min) 6 mg kg^{-1}, vitamin B_6 (min) 3 mg kg^{-1}, vitamin B_{12} (min) 9 mg kg^{-1}, folic acid (min) 1 mg kg^{-1}, pantothenic acid (min) 12 mg kg^{-1}, biotin (min) 0.5 mg kg^{-1}, choline (min) 500 mg kg^{-1}, niacin (min) 20 mg kg^{-1}, Cu (min) 9 mg kg^{-1}, Fe (min) 40 mg kg^{-1}, I (min) 1 mg kg^{-1}, Mn (min) 90 mg kg^{-1}, Se (min) 0.4 mg kg^{-1}, and Zn (min) 50 mg kg^{-1}. Lanthanum was determined in food and water, and the concentration was lower than 0.03 μg g^{-1} and 0.01 μg L^{-1}. The study was approved by the Animals Ethics Committee of the university (protocol number 4250170317).

2.3 Treatment of Animals for Chronic Toxicity Study of La_2O_3NPs

Chronic toxicity of La_2O_3NPs was discovered after a 7-day stabilization period. The animals were randomly divided into four groups as follows: group 1 (10 rats) served as the control group (CTR), group 2 (10 rats) received 1.0 mg kg^{-1} of La_2O_3NPs per body weight (T1), group 3 (10 rats) received 10.0 mg kg^{-1} of La_2O_3NPs per body weight (T2), and group 4 (10 rats) received 100 mg kg^{-1} of La_2O_3NPs per body weight (T3). A constant volume of NPs suspension was used once daily for 30 days, 5 days a week, at dose equivalents of 1.0, 10.0, and 100 mg kg^{-1} body weight. Every animal was weighed once a week. The vehicle (water) was given to the control animals in a single dose only. All solutions were given by gavage in a volume of 1.0 mL kg^{-1} body and between 04 pm and 05 pm. The animals were weighed after treatment and euthanized with halothane (1-bromo-1-chloro-2,2,2-trifluoroethane). Femur bones were extracted for further research. The femurs were promptly preserved at -20°C until they were analyzed.

2.4 Preparation of Bone for Analysis

The male Wistar rats' femoral bone was thawed at room temperature and then dried to a consistent weight at 105 °C. The dry materials were pulverized in an agate mortar until the granulometry was less than 100 m for total element determination. The thawed femur was sliced using a saw and then sanded to a flat smooth homogeneous surface for LA-ICP-MS analysis. The epiphyseal line was cut cross sectional through the bone's head. A 2 mm thick slice of bone sample was then glued to a glass slice and ablated directly. One line was ablated twice to assess potential contamination from the sample preparation technique. The signal strength of the elements was identical at the first and second ablations (surface of the sample), indicating that no major contamination occurred.

2.5 Instrumentation and Measurement Procedure

LA-ICP-MS measurements were carried out with the help of a CETAC LSX-266 (at 266 nm) LA system (Cetac Technologies, Inc., USA) linked to a PerkinElmer ELAN DRCII apparatus. With changes, the laser ablation parameters described by Vašinová Galiová and co-authors [41] for spatially resolved analysis were used.

To obtain images of element distribution, multiple line modes were used to ablate the bone

samples. The laser beam's resolution (spot size) was set to 100 μm, and the laser's speed was set to 100 μm s^{-1}. The ablation lines were separated by 10 μm. LA-ICP-MS measurements were carried out with the help of a CETAC LSX-266 (at 266 nm) LA system (Cetac Technologies, Inc., USA) linked to a PerkinElmer ELAN DRCII apparatus. With changes, the laser ablation parameters described by Nunes and co-authors [42] for spatially resolved analysis were used. To obtain images of element distribution, multiple line modes were used to ablate the bone samples. The laser beam's resolution (spot size) was set to 100 μm, and the laser's speed was set to 100 μm s^{-1}. The ablation lines were separated by 10 μm.

2.6 Statistical Analysis of the Results

One-way ANOVA was used to evaluate the data acquired for the control and treatment groups. The data were previously assessed in terms of their distribution, and it was discovered that they follow a normal distribution. All results were given as the mean and standard deviation (mean SD). To confirm the significance of positive responses, multiple pairwise comparisons were performed using Dunnett's multiple comparison post-test and Student's 't' test. Graph Pad Instat Prism 3 Software package for Windows (Graph Pad Software, Inc., La Jolla, CA, USA) was used for statistical analysis. For all tests, the statistical significance level was set at P 0.05.

Table 1 Operating conditions for ICP-MS, LA-ICP-MS, and ICP OES instrument

Parameters	ICP-MS	LA-ICP-MS	ICP OES
RF power, W	1300	1300	1400
Plasma gas flow, L min^{-1}	15	15	15
Auxiliary Argon flow, L min^{-1}	1.2	1.2	0.20
Nebulizer Argon flow, L min^{-1}	1.10	1.30	0.70
Dwell time, ms	40	20	-
Sweeps per reading	5	1	-
Reading per replicate	5	Variable	-
Replicates	3	1	3
Isotope monitored, m/z	^{139}La,^{55}Mn,^{65}Cu,^{13}C, ^{82}Se,^{98}Mo	^{23}Na,^{26}Mg,^{27}Al,^{31}P, ^{32}S,^{39}K,^{43} Ca,^{55}Mn, ^{56}Fe,^{63}Cu,^{66}Zn,^{87} Sr, ^{138}Ba,^{139}La	-
Wavelengths, nm	-	-	Ca(393), Fe(238), K(766), Mg(285), P(214), Zn(206)
Carrier gas flow rate, L-min^{-1}	-	1.30	-
Ablation cell volume,-mL	-	50	-
Ablation frequency, Hz	-	20	-
Spot size, μm	-	100	-
Fluency, J cm^{-2}	-	11.9	-

Scan rate, μm s^{-1}	-	100	-
Pulse width, μm	-	5	-
Ablation method	-	Single and multiline	

3.0 Results

Table 2 compares the Ca-normalized Ni, Zn, Cu, Sr, and Ba ratios of the control group (CTR) to the values obtained in (T1), (T2), and (T3).

Table 2: The Ca-normalized Mn, Zn, Cu, Sr, Ba, and Pb ratios of the control group (CTR) standard were determined, and the results were obtained in 1.0 mg kg^{-1} of La_2O_3NPs per body weight (T1), 10.0 mg kg^{-1} of La_2O_3NPs per body weight (T2), and 100 mg kg^{-1} of La_2O_3NPs per body weight (T3).

	Mn/Ca	Zn/Ca	Cu/Ca	Sr/Ca	Ba/Ca	Pb/Ca
Average ratio in the control sample (CTR).	3×10^{-4}	5.6×10^{-4}	3.0×10^{-4}	1.1×10^{-4}	1.5×10^{-4}	3.8×10^{-4}
Average ratio in the treatment I (T1)	3.3×10^{-4}	4.7×10^{-4}	3.1×10^{-4}	2.0×10^{-4}	3.4×10^{-4}	1.0×10^{-4}
Average ratio in the treatment II (T2)	4.2×10^{-4}	4.6×10^{-4}	2.6×10^{-4}	2.7×10^{-4}	3.9×10^{-4}	2.9×10^{-4}
Average ratio in the treatment III (T3)	3.9×10^{-4}	2.1×10^{-4}	4.2×10^{-4}	2.2×10^{-4}	2.1×10^{-4}	2.8×10^{-4}

Strontium was found in all bones at the Ca-normalized Sr ratio (Table 2), with a significantly greater value found in the femur bone of the male Wistar rat treated with 10.0 mg kg^{-1} La_2O_3NPs (T2). The distribution of characteristics in the Sr map of the control and T3 femur bone heads observed is distinct and significantly more homogeneous, as demonstrated in Figures 1 and 4. The Sr concentration in CTR rats was lower than in T1 and T2. Strontium concentrations in bone T2 show a distinct fluctuation, which is visible as a yellow-colored zone, correlating to a higher concentration of Sr, which corresponds to an $^{87}Sr/^{43}Ca$ rat

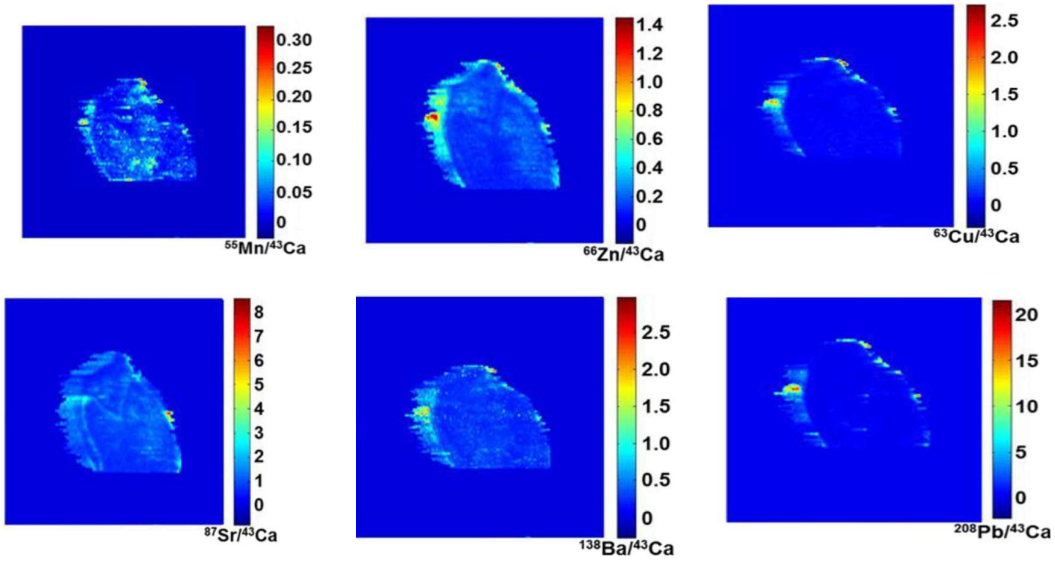

Fig. 1. Images of Mn, Zn, Cu, Sr, Ba, and Pb ions of control male wistar rat femur head bone measured by LA-ICP-MS

larger than around 20, as shown in Fig. 1. The Ca-normalized Zn ratio was lower in the bones of NP-treated animals than in the control sample. Figures 1–4 illustrate that the highest Zn concentrations were found along the bone's outer edge, with the inside region of the bone head having very low amounts. Zinc concentrations in bone T3 show a distinct fluctuation, which is visible as a yellow-colored zone, correlating to a lower concentration of Zn, which corresponds to a $^{66}Zn/^{43}Ca$ ratio less than 2.1, as seen in Fig. 4. The increased quantity of the element Pb was found solely on the bone's surface (Figures 2–4). Table 3 shows that Pb is distributed in the following order using the ratio $^{208}Pb/^{43}Ca$: T1 T3 T2 CTR.

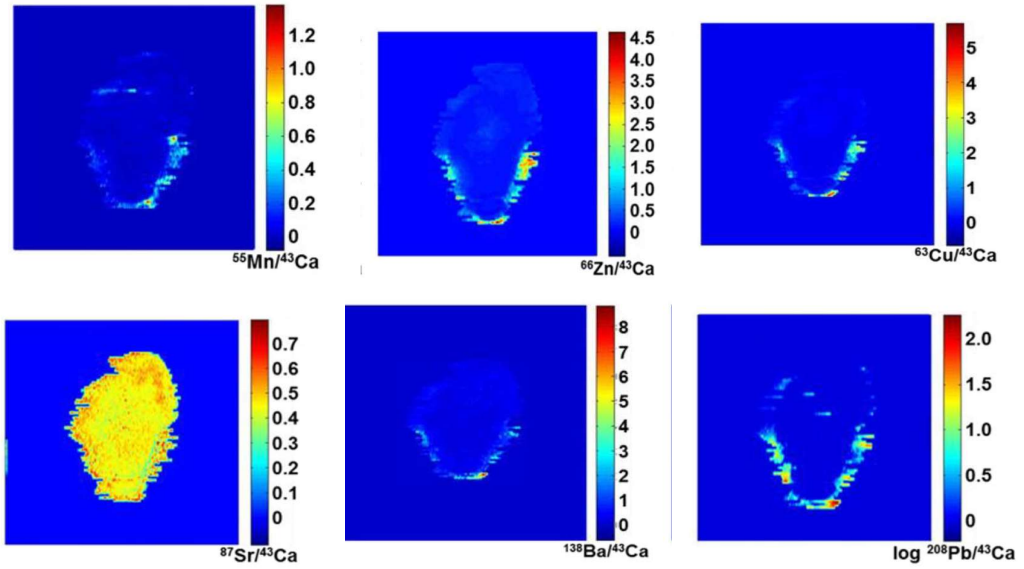

Fig. 2. Images of Mn, Zn, Cu, Sr, Ba, and Pb ions of 1.0 mg kg^{-1} of La_2O_3NPs per body weight (T1) male wistar rat femur head bone measured by LA-ICP-MS

Figures 1–4 show the geographical distribution of Mn in a cross section of the treated femur bone heads and control sample, as measured by the LA-ICP-MS ratio of $^{55}Mn/^{43}Ca$. The Mn concentration of the femur bone head cross section differed significantly within and between animal groups. The outer areas of samples T1, T2, and T3 are richer relative to the center areas, according to ablation pictures. There are also many sites with very increased Mn deposits.

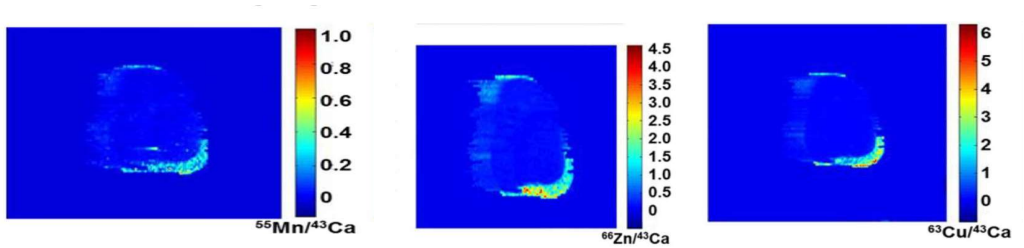

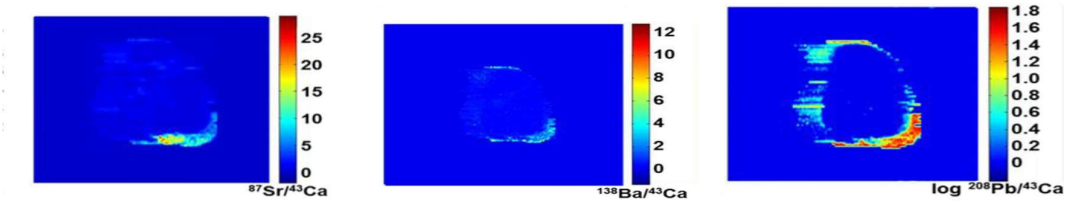

Fig. 3. Images of Mn, Zn, Cu, Sr, Ba, and Pb ions of 10.0 mg kg^{-1} of La_2O_3NPs per body weight (T2) male wistar rat femur head bone measured by LA-ICP-MS

Cu spatial elemental distribution patterns in ablated femur bone head demonstrate significant variation within regions and diverse element distributions. The outer portions of the bone sample had higher normalized intensities of the $^{63}Cu/^{43}Ca$ than the core region. The Ca-normalized Cu ratios were found to be lowest in T2 (2.6 $x10^{-6}$) and greatest in T3 (4.2 $x10^{-6}$) as shown in Table 2.

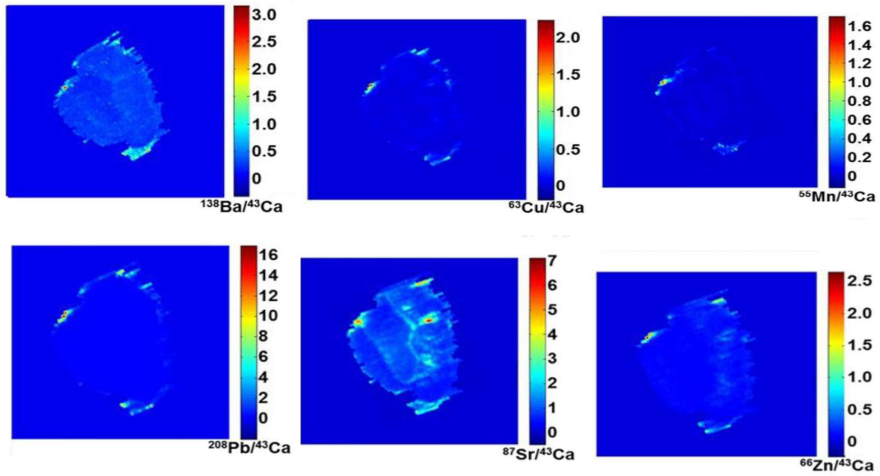

Fig. 4. Images of Mn, Zn, Cu, Sr, Ba, and Pb ions of 100.0 mg kg^{-1} of La_2O_3NPs per body weight (T3) male wistar rat femur head bone measured by LA-ICP-MS

Figures 1–4 show the geographical distribution of Ba in a cross section of the treated femur bone heads and control sample, as measured by the LA-ICP-MS $^{138}Ba/^{43}Ca$ ratio. The amount of Ba in the femur bone head cross section differed significantly among and across groups of animals. Figures 1–4 show that the periphery areas of samples T1, T2, and T3 are richer compared to the center areas. There are also multiple places with sharply elevated Ba deposits, and as shown in Table 2, the values of the Ca-normalized Ba ratios were lowest in T3 (2.1 $x10^{-4}$) and greatest in T2 (3.9 $x10^{-4}$).

There were no significant differences in Mn/Ca ratios between T1, T2, and T3 femur head bone of the male wistar rat (P = 0.5509, Fig.5). This is most likely owing to the male Wistar rat's femur bone's extremely low Mn level. The Zn/Ca ratios in the femur bone head of male wistar rats treated with 10 mg/kg and 1 mg/kg La_2O_3NP are higher than in the other treatments (P =0.0319, Fig. 5). In contrast, the Cu/Ca ratios are lower in male wistar rat femur bone heads treated with 10 mg/kg La_2O_3NP than in other treatments (P = 0.0833, Fig. 5), and the Sr/Ca ratios do not differ among male wistar rat femur bone heads (P = 0.7216, Fig. 5).

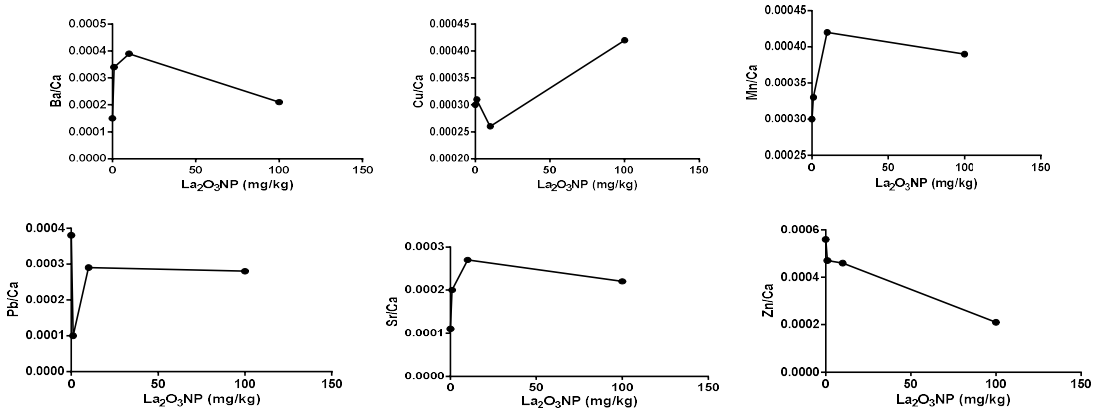

Fig. 5. Correlations between Ca content and levels of the trace elements Ba, Cu, Mn, Pb, Sr and Zn in the La_2O_3NP treated femoral head bone of male wistar rat measured by LA-ICP-MS.

There is no sign for the Mn/Ca ratios.T1 and T2 Ba/Ca ratios are similar (P = 0.6905, Fig. 5). However, the femur bone head of male wistar rats treated with 100 mg/kg La_2O_3NP was lower. There were no significant differences in Pb/Ca ratios between T2 and T3 femur head bone of the male wistar rat (P = 0.8906, Fig.5). This is most likely owing to the male Wistar rat's femur bone's extremely low Mn level.

4.0 Discussion

4.1 Variations between La_2O_3NP treated femoral head bone of male wistar rat measured by LA-ICP-MS

The purpose of this work was to determine the geographical distribution of trace element ca-normalized ratios in the bone of male wistar rats following acute oral administration of La_2O_3NPs.

The absorption of La_2O_3NPs can be attributed to the fact that some of them exist as agglomerates [43]. The effects of oral administration of La_2O_3NPs on the spatial distribution of trace element ca-normalized ratios in male wistar rats' femur bone were studied. The bone matrix is reported to be 90% hydroxyapatite ($Ca_{10}[PO_4]_6[OH]_2$), with Ca, P, and much less Mg as significant ingredients. Furthermore, the bone elements K and Na, which are closely related to Ca metabolism, as well as Mn, Cu, and Zn, are co-factors for enzymes [44].

The differences in the Zn/Ca ratio between T1, T2, and T3 femur bone of male Wistar rats for a given profile are not significant, but this is owing to a small number of analyses (Fig 5). In the case of Zn, taking the entire data-set into account does not improve the statistics since it combines low Zn/Ca values in "T3" profiles with high Zn/Ca values in "T1" and "T2" profiles (Fig. 5) [45]

In T1, T2, and T3, the transition metals Ni and Cu have lower and larger Ca normalized ratios, respectively. Transition metals are bio-essential elements that are metabolically controlled, therefore no concentration changes are predicted in normal/healthy conditions [46]. The fact that the Ni/Ca and Cu/Ca ratios alter between T1, T2, and T3 femur head bone suggests that the metabolic control of Ni and Cu differs when La_2O_3NPs are administered orally. In femur

head bone, the alkaline metals Sr and Ba, which have equivalent electrical characteristics as Ca, have lower Ca normalized ratios in T1, T2, and T3.

4.2 Ca-biopurification in femur bone

Ca-biopurification reflects the favorable component through which Sr and Ba decrease in transferring Ca via physiological reactions [47]. According to the [48] study, the Sr/Ca and Ba/Ca ratios decrease in animals with climbing trophic position. The Sr/Ca and Ba/Ca ratios in bone vary linearly at the trophic chain size when expressed in log scale, showing that the Ca-biopurification process of Sr and Ba between two successive trophic steps is related by a power law [49].

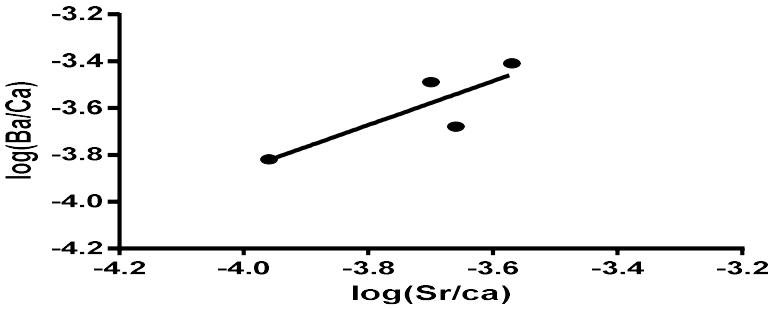

Fig. 6. Variations of the Sr/Ca and Ba/Ca ratios in the La_2O_3NP treated femoral head bone of male wistar rat measured by LA-ICP-MS expressed in log scale.

According to the findings of this study, the Ca-biopurification process of Sr and Ba in La_2O_3NP treated femur head bone follows the same power law (Fig. 5). The finding that the Ca-biopurification mechanism in bone is equivalent has two major implications. The first point to mention is that the Sr partitioning coefficients in bone are similar. This is also true for Ba, extending the conclusions of Balter and Lécuyer [50] to the 37 °C temperature.

Conclusions

LA-ICP-MS is an effective approach for bio-imaging trace elements in bone, however the information encoded in the bone's intricate structure is difficult to decode. LA-ICP-MS was utilized to evaluate Ca-normalized trace element ratios along profiles of the femur bone head after rats were given La_2O_3NPs for 30 days. It was found that some systematic differences between the values obtained in 1.0 mg kg^{-1} of La_2O_3NPs per body weight (T1), 10.0 mg kg^{-1} of La_2O_3NPs per body weight (T2), 100 mg kg^{-1} of La_2O_3NPs per body weight (T3), notably for the Cu/Ca, Mn/Ca, Zn/Ca, Sr/Ca, Pb/Ca and Ba/Ca ratios, reflecting the in utero incorporation of the elements. The treated femur bone head also had a higher Zn content than the other elements. This finding is significant in developmental biology because it can translate some chemical cues that inhibit bone growth. Taking all of these findings into consideration, the study recommends that one raster along the femur bone head will most likely blend all of the chemical information.

Acknowledgments

The authors would like to express their gratitude to the Conselho Nacional de Desenvolvimento Cientifico e Tecnológico (CNPq, Proc. Nr. 120230/2017-8 and Proc. Nr. 306052/2017-2) and Afe Babalola University Ado-Ekiti Nigeria for providing scholarships and funding for this project.

Compliance with Ethical Standards

The Animals Ethics Committee of the Federal University of Santa Maria (CEUA, protocol number 4250170317) approved all techniques used in animal investigations. CEUA adheres to the criteria of the Conselho Nacional de Controle de Experimentaço Animal (CONCEA), Brazil's Guide for the Production, Maintenance, or Use of Animals for Teaching or Scientific Research Activities.

Conflict of Interest

The authors declare that they have no conflict of interest.

Reference

[1]. Rodríguez-Estival J., Álvarez-Lloret P., Rodríguez-Navarro A.B., Mateo R, "Chronic effects of lead (Pb) on bone properties in red deer and wild boar: relationship with vitamins A and D3". *Environmental Pollution* , 2013, 174, 142–149. DOI: 10.1016/j.envpol.2012.11.019

[2]. Sobczak-Kupiec A., Malina D., Kijkowska R., Wzorek Z, "Comparative Study of Hydroxyapatite Prepared by the Authors with Selected Commercially Available Ceramics," *Digest Journal of Nanomaterials and Biostructures*, 2012, 7, No 1, 385 – 391.

[3]. Kourkoumelis N., Balatsoukas I., Tzaphlidou M, "Ca/P concentration ratio at different sites of normal and osteoporotic rabbit bones evaluated by Auger and energy dispersive X-ray spectroscopy". *Journal of Biol. Phys*, 2012, 38; 279– 291. DOI: 10.1007/s10867-011-9247-3

[4]. Sprio S., Preti L., Montesi M., Panseri S., Adamiano A., Vandini A, "Surface phenomena enhancing the antibacterial and osteogenic ability of nanocrystalline hydroxyapatite, activated by multiple-ion doping". ACS Biomater. Sci. Eng, 2019, 5, 5947–5959. DOI: 10.1021/ acsbiomaterials.9b00893

[5]. Tite T., Popa A.C., Balescu L.M., Bogdan I.M., Pasuk I., Ferreira J.M.F., Stan G.E, "Cationic substitutions in hydroxyapatite: current status of the derived bio-functional effects and their in vitro interrogation methods," Materials, 2018, 11, E2081. DOI: 10.3390/ma11112081

[6]. Garbo C., Locs J., D'Este M., Demazeau G., Mocanu A., Roman C., Horovitz O., Tomoaia-Cotisel M, "Advanced Mg, Zn, Sr, Si multi-substituted hydroxyapatites for bone regeneration". *Int. Journal Nanomed*, 2020, 15, 1037-1058. DOI https://doi.org /10.2147/IJN.S226630

[7]. Montazeri L., Javadpour J., Shokrgozar M. A., Bonakdar S., Javadian S, "Hydrothermal synthesis and characterization of hydroxyapatite and fluorhydroxyapatite nano-size

powders," *Biomedical Materials*, 2010, 5(4), 045004. DOI:10.1088/1748-6041/5/4/045004.

[8]. Weatherholt A. M., Fuchs R. K., Warden S. J., "Specialized connective tissue: bone, the structural framework of the upper extremity," *Journal of Hand. Ther*. 2012, 25, 123–131. DOI: 10.1016/j.jht.2011.08.003

[9]. Wang L., Yu H., Yang G., Zhang Y., Wang W., Su T., Ma W., Yang F., Chen L., He L, "Correlation between bone mineral density and serum trace element contents of elderly malesin Beijing urban area". *Int. Journal of Clin. Exp. Med*, 2015, 8: 19250.

[10]. He X., Zhang Z. Y., Feng L. X., Li Z. J., Yang J. H., Zhao Y. L., Chai Z. F., "Effects of acute lanthanum exposure on calcium absorption in rats," *Journal of Radioanalytical and Nuclear Chemistry volume*, 2007, 272, 557–559. https://doi.org/10.1007/s10967-007-0623-1

[11]. Carafoli E., Lim D., "Plasma Membrane Calcium ATPase," *Handbook of Neurochemistry and Molecular Neurobiology*, 2009, 581–596. DOI: 10.1007/978-0-387-30370-3_32

[12]. Liu B., Zhang B., Huang S., Yang L., Roos C. M., Thompson M. A., Prakash Y.S., Zang J., Miller J.D., Guo R., "Ca^{2+} Entry through reverse mode Na^{+}/Ca^{2+} Exchanger contributes to store operated channel-mediated neointima formation after arterial injury," *Canadian Journal of Cardiology*, 2018, 34:791–799.

[13]. Arora M., Hare D., Austin C., Smith D.R., Dobl P., "Spatial distribution of manganese in enamel and coronal dentine of human primary teeth," *Sci. Total Environ*. 409, 1315–1319, 2011. DOI: 10.1016/j.scitotenv.2010.12.018

[14]. Asaduzzaman K., Khandaker M.U., Baharudin N.A.B., Bin Mohd Amin Y., Farook M.S., Bradley D.A., Mahmoud O., "Heavy metals in human teeth dentine: a bio-indicator of metals exposure and environmental pollution," *Chemosphere*, 2017, 176, 221–230. DOI: 10.1016/j.chemosphere.2017.02.114

[15]. Wilschefski S. C., Baxter M. R., "Inductively Coupled Plasma Mass Spectrometry: Introduction to Analytical Aspects," *Clin Biochem Rev*, 2019, 40, 3, 115-133. DOI: 10.33176/AACB-19-00024

[16]. Dolphin A. E., Goodman A. H., Amarasiriwardena D. D., "Variation in elemental intensities among teeth and between pre- and postnatal regions of enamel," *American Journal of Physical Anthropology*, 2005, 128, 4, 878–888. https://doi.org/10.1002/ajpa.20213

[17]. Shepherd T. J., Dirks W., Roberts N. M. W., Patel J. G., Hodgson S., Pless-Mulloli T., Walton P., Parrish R.R., "Tracing fetal and childhood exposure to lead using isotope analysis of deciduous teeth. Environ," Res., 2016, 146, 145–153. DOI: 10.1016/j.envres.2015.12.017

[18]. Austin C., Smith T. M., Bradman A., Hinde K., Joannes-Boyau R., Bishop D., Hare D.J., Doble P., Eskenazi B., Arora M., "Barium distributions in teeth reveal earlylife dietary transitions in primates. *Nature*, 2013, 498, 216–219. DOI: 10.1038/nature12169

[19]. Guede I., Zuluaga M.C., Ortega L.A., Alonso-Olazabal A., Murelaga X., Pina M., Gutierrez F.J., "Analyses of human dentine and tooth enamel by laser ablation-inductively coupled plasma-mass spectrometry (LA-ICP-MS) to study the diet of

medieval Muslim individuals from Tauste (Spain)," *Microchem. Journal,* 2017, 130, 287–294. DOI:10.1016/j.microc.2016.10.005

[20]. Kohn M.J., Moses R.J., "Trace element diffusivities in bone rule out simple diffusive uptake during fossilization but explain in vivo uptake and release," *Proc. Natl. Acad. Sci. U. S. A.*, 2013, 110, 419–424. DOI: 10.1073/pnas.1209513110

[21]. Vašinová G. M., Nývltová F. M., Kynický J., Prokeš L., Neff H., Mason, A.Z., Gadas P., Košler J., Kanický V., "Elemental mapping in fossil tooth root section of Ursus arctos by laser ablation inductively coupled plasma mass spectrometry (LAICP- MS)," *Talanta*, 2013, 105, 235–243. DOI: 10.1016/j.talanta.2012.12.037

[22]. Le Roux P. J., Lee-Thorp J., Copeland S.R., Sponheimer M., de Ruiter D.J., "Strontium isotope analysis of curved tooth enamel surfaces by laser-ablation multi-collector ICP-MS," *Palaeogeogr. Palaeoclimatol. Palaeoecol*, 2014 416, 142–149. https://doi.org/10.1016 /j.palaeo.2014.09.007

[23]. Copeland S.R., Sponheimer M., de Ruiter D.J., Lee-Thorp J.A., Codron D., Le Roux P.J., Grimes V., Richards M.P., "Strontium isotope evidence for landscape use by early hominins," *Nature*, 2011, 474, 76–79. DOI: 10.1038/nature10149

[24]. Balter V., Braga J., Télouk P., Thackeray F., "Evidence for dietary change but not landscape use in South African early hominins," *Nature*, 2012, 489, 558–560. DOI: 10.1038/nature11349

[25]. Arora M., Hare D., Austin C., Smith D.R., Doble P., "Spatial distribution of manganese in enamel and coronal dentine of human primary teeth," *Sci. Total Environ*., 2011, 409, 1315–1319.

[26]. Vašinová G. M., Nývltová F. M., Kynický J., Prokeš L., Neff H., Mason A.Z., Gadas P., Košler J., Kanický V., "Elemental mapping in fossil tooth root section of Ursus arctos by laser ablation inductively coupled plasma mass spectrometry (LAICP- MS)," *Talanta*, 2013 105, 235–243.

[27]. Nunes M.A.G., Voss M., Corazza G., Flores E.M.M., Dressler V.L., "External calibration strategy for trace element quantification in botanical samples by LA-ICP-MS using filter paper," *Anal Chim Acta*, 2016, 905: 51–57.

[28]. Qu X., He Z., Qiao H., Zhai Z., Mao Z., Yu Z., Dai K., "Serum copper levels are associated with bone mineral density and total fracture," *Journal Orthop Translat*, 2018, 31, 14, 34-44.

[29]. Guede I., Zuluaga M. C., Ortega L. A., Alonso-Olazabal A., Murelaga X., Pina M., Gutierrez F. J., "Analyses of human dentine and tooth enamel by laser ablation-inductively coupled plasma-mass spectrometry (LA-ICP-MS) to study the diet of medieval Muslim individuals from Tauste (Spain)," *Microchemical Journal*, 2017 130, 287–294.

[30]. Rasmussen K. L., Milner G. R., Skytte L., Lynnerup N., Thomsen J. L., Boldsen J. L., "Mapping diagenesis in archaeological human bones," *Herit Sci*, 2019 7: 41.

[31]. Lugli F., Brunelli D., Cipriani A., Bosi G., Traversari M., Gruppioni G., "C_4-plant foraging in northern Italy: stable isotopes, Sr/Ca and Ba/Ca data of human osteological samples from Roccapelago (16th–18th centuries AD)," *Archaeometry*, 2017, 59: 1119–34.

[32]. Robles-Linares J. A., Winter K., Liao Z., "The Effect of Laser Ablation Pulse Width and Feed Speed on Necrosis and Surface Damage of Cortical Bone," *Chin. J. Mech. Eng*, 2022, 35, 52.

[33]. Eliceiri K. W., Berthold M. R., Goldberg I. G., Ibáñez L., Manjunath B.S., Martone M. E., Murphy R. F., Peng H., Plant A. L., Roysam B., Stuurman N., Swedlow J. R., Tomancak P., Carpenter A. E., "Biological imaging software tools," *Nat Methods*, 2012, 28, 9, 7, 697-710.

[34]. Padovani F., Mairhörmann B., Falter-Braun P., "Segmentation, tracking and cell cycle analysis of live-cell imaging data with Cell-ACDC," *BMC Biol,* 2022, 20, 174.

[35]. Caicedo J., Cooper S., Heigwer F., "Data-analysis strategies for image-based cell profiling," *Nat Methods*, 2017 14, 849–863.

[36]. Nunes M.A.G., Voss M., Corazza G., Flores E.M.M., Dressler V.L., "External calibration strategy for trace element quantification in botanical samples by LA-ICP-MS using filter paper," *Anal Chim Acta*, 2016, 905:51–57.

[37]. Yao W., Guangsheng G., Fei W., Jun W., "Fluidization and agglomerate structure of SiO2 nanoparticles," *Powder Technol*, 2002 124, pp. 152-159.

[38]. Wang H., Zhou T., Yang J. S., Wang J. J., Kage H., Mawatari Y, "Model for calculation of agglomerate sizes of nanoparticles in a vibro-fluidized bed," *Chem. Eng. Technol*, 2010, 33, 388-394.

[39]. Feng X., "Chemical and Biochemical Basis of Cell-Bone Matrix Interaction in Health and Disease," *Curr Chem Biol*, 2009, 1, 3, 2, 189-196.

[40]. Gomes D. S., Santos A. M. C., Neves G. A., Menezes R. R., "A brief review on hydroxyapatite production and use in biomedicine," *Cerâmica*, 2019, 65, 282-302.

[41]. Vašinová G. M., Nývltová F. M., Kynický J., Prokeš L., Neff H., Mason A.Z., Gadas P., Košler J., Kanický V., Elemental mapping in fossil tooth root section of Ursus arctos by laser ablation inductively coupled plasma mass spectrometry (LAICP- MS). *Talanta*, 2013, 105, 235–243.

[42]. Nunes M.A.G., Voss M., Corazza G., Flores E.M.M., Dressler V.L., External calibration strategy for trace element quantification in botanical samples by LA-ICP-MS using filter paper. *Anal Chim Acta*, 2016, 905:51–57.

[43]. Rastogi V., Velev O. D., Development and Evaluation of Realistic Microbioassays in Freely Suspended Droplets on a Chip. *Biomicrofluidics*, 2007, 1, 17.

[44]. Dermience M., Lognay G., Mathieu F., Goyens P., Effects of thirty elements on bone metabolism. *Journal Trace Elem Med Biol*, 2015, 32, 86–106.

[45]. Nie K., Zhu Z., Munroe P., The effect of Zn/Ca ratio on the micro-structure, texture and mechanical properties of dilute Mg–Zn–Ca–Mn alloys that exhibit superior strength. *J Mater Sci*, 2020, 55, 3588–3604. https://doi.org/10.1007/s10853-019-04174-4.

[46]. Reynard B., Balter V., Trace elements and their isotopes in bones and teeth: diet, environments, diagenesis, and dating of archaeological and pale-ontological samples. *Palaeogeogr. Palaeoclimatol. Palaeoecol*, 2014, 416, 4–16.

[47]. Wasserman R.H., Comar C.L., Papadopoulou D. Dietary calcium levels and reat retention of radio strontium in the growing rat. *Science*, 1957, 126, 1180–1182.

[48]. Elias R.W., Hirao Y., Patterson C.C., The circumvention of the natural bio-purification of calcium along nutrient pathways by atmospheric inputs of industrial lead. Geochim. Cosmochim. *Acta*, 1982, 46, 2561–2580.

[49]. Balter V., Allometric constraints on Sr/Ca and Ba/Ca partitioning in terrestrial trophic chains. *Oecologia*, 2004, 139, 83–88.

[50]. Balter V., Lécuyer C., Determination of Sr and Ba partition coefficients between apatite from fish (Sparus aurata) and seawater: the influence of temperature. Geochim. Cosmochim. *Acta*, 2010, 74, 3449–3458.